CHINESE JOURNAL OF PHYSICS VOL. 33, NO. 3 JUNE 1995

Josephson Effects on $YBa_2Cu_3O_y$ Junctions and SQUID†

H. C. Yang, J. H. Lu, L. C. Ku, and H. M. Cho
Department of Physics, National Taiwan University, Taipei, Taiwan 106, R.O.C.

H. E. Horng
Department of Physics, National Taiwan Normal University, Taipei, Taiwan 106, R.O.C.

(Received March 9, 1995)

Characteristics of $YBa_2Cu_3O_y$ step-edge and bi-epitaxial Josephson junctions and SQUID's are reported. Current-voltage ($I-V$) curves show the behavior predicted according to a model of a resistively shunted junction (RSJ). The $I-V$ curves under microwave irradiation show constant voltage steps; the amplitude of the constant voltage steps is modulated by the microwave power. The RSJ current-source model is used to discuss the $I-V$ curves under microwave irradiation and applied magnetic fields. The $V-\Phi$ curves of the SQUID's show modulation up to 77 K.

PACS. 74.50.+r – Proximity effects, weak links, tunneling phenomena, and Josephson effects.

I. INTRODUCTION

High-T, Josephson junctions and SQUID's are of current interest because of the potential application of these devices at 77 K. Much research [1-9] was focused on the fabrication and characterization of junctions and SQUID's. In this work we report on the characteristics of $YBa_2Cu_3O_y$ (YBCO) step-edge and bi-epitaxial Josephson junctions and SQUID's. Current-voltage (I-V) curves show the behavior predicted according to a model of a resistively shunted junction (RSJ). The I-V curves under microwave irradiation show constant-voltage steps; the amplitude of the constant-voltage steps is modulated by microwave power. The current-source model of an RSJ is used to discuss the I-V curves of the junctions and SQUID's under microwave irradiation and magnetic fields.

† Refereed version of the invited paper presented at the Annual Meeting of the Physical Society of R.O.C., January 19-20, 1995.

II. EXPERIMENTAL SECTION

YBCO step-edge Josephson junctions and SQUID's were prepared according to standard techniques of photo-lithography and ion milling. (001) oriented MgO substrates were etched to a stepedge with a height of 1500-3000 A. During ion milling, the direction of the ion beam was perpendicular to the stepedge and made an angle of $\sim 60°$ with respect to the normal of the MgO substrate shown in Fig. la. The incident energy of the beam of Ar^+ ions was 500 eV and the distance from the ion source to the substrate was about 10 cm. We grew YBCO films 1500-2500 Å thick onto the MgO (001) substrate with and without stepedges. The YBCO films grown on the MgO substrates have $T_{c,zero} \sim$ 85-88 K whereas the $T_{c,zero}$ of the YBCO films on the MgO substrates with a stepedge were 83 $\sim$ 86 K. The YBCO films were patterned to the Josephson junctions or the SQUID's shown in Fig. lb for $I-V$ measurements. The junction width varied from 5 to 40 μm and the hole area of the SQUID's varied from 5 x 5 to 20 x 20 μm^2.

Bi-epitaxial YBCO Josephson junctions fabricated on the CeO_2/MgO (001) substrates shown in Fig. 2 were prepared by depositing an epitaxial layer of CeO_2 film 200 $\sim$ 300 Å thick onto the (001) oriented MgO substrates with a magnetron sputtering system. The sputtering target was CeO_2 with a diameter of 50 mm. CeO_2 films were grown at about 700 $\sim$ 750 °C. The sputtering gas was a mixture of Ar and O_2(3:7) and the sputtering pressure was 200 $\sim$ 300 mtorr. After growth, O_2 at 1 atm was introduced into the vacuum chamber. The films were kept at 600 °C for an hour and then cooled to

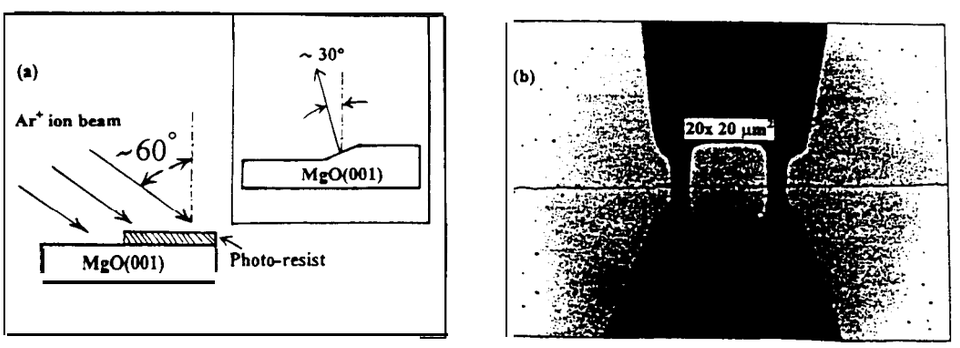

FIG. 1. (a) Orientation of Ar^+ ion beams with respect to the photo-resist on a (001) orinted MgO substrate, the direction of the ion beam is perpendicular to the step-edge of the photo-resist and makes an angle of 60" with respect to the normal of the MgO substrate. (b) Geometrical configuration of a patterned step-edge YBCO SQUID, the SQUID has a hole area of 20 x 20 μm^2 and the junction width was 5 μm.

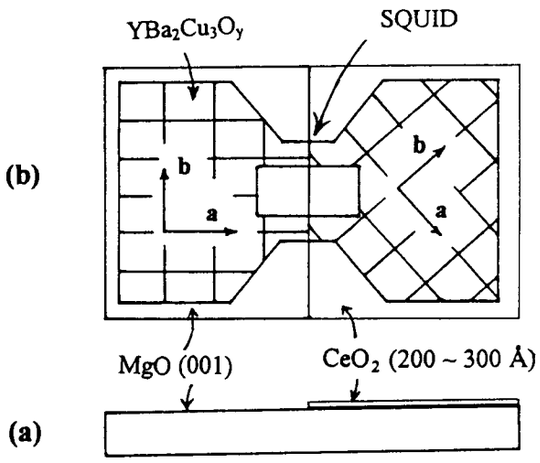

FIG. 2. (a) CeO_2/MgO (001) substrate in which half the (001) oriented MgO substrate was covered with a thin CeO_2 layer (200 ~ 300 Å thick). (b) YBCO SQUID fabricated from bi-epitaxial YBCO films on a CeO_2/MgO (001) substrate shown in Fig. 1a.

room temperature at a rate 5 °C per minute. For junction and SQUID fabrication, CeO_2/MgO (001) substrates were ion-milled to a pattern so that half the MgO (001) substrate was covered with CeO_2 (Fig. 2a). The YBCO films were grown onto the CeO_2/MgO (001) substrates. Josephson junctions and SQUID's (Fig. 2b) were fabricated using bi-epitaxial YBCO films on CeO_2/MgO (001) substrates. The junction width was 10-20 μm wide.

Gold pads were deposited on the electrical leads of the junctions or the SQUID's. Current-voltage ($I-V$) curves with and without microwave irradiation were measured at various temperatures to characterize the junction behavior. The microwaves were coupled to the junction with a dipole antenna. The magnetic fields were applied to the SQUID's via a solenoid. The samples were shielded with two layers of mu-metal. The temperature of the sample was monitored with calibrated silicone diode.

III. RESULTS AND DISCUSSION

Figure 3 shows a typical $I-V$ curve for a step-edge Josephson junction at 65 K. The $I-V$ curves follow the prediction of the resistive shunted junction model. There was no hysteresis in these $I-V$ curves.

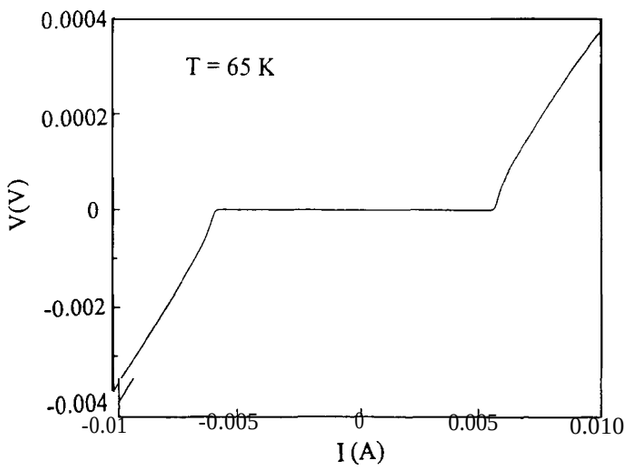

FIG. 3. Z $-V$ curve for a step-edge junction at $T = 65$ K.

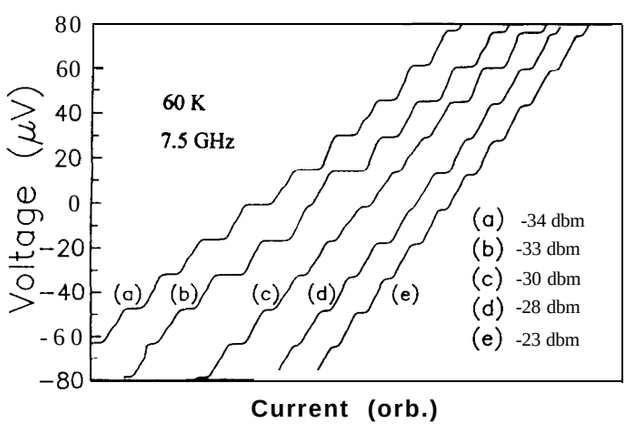

FIG. 4. Z − V curves for a step-edge Josephson junction under microwave irradiation at $T = 60$ K and $f = 7.5$ GHz. The Z − V curves reveal constant-voltage steps that are modulated by the microwave power.

Figure 4 shows $I-V$ curves for a step-edge Josephson junction under microwave irradiation at T = 60 K and $f = 7.5$ GHz. The $I-V$ curves reveal constant-voltage steps; the constant-voltage steps follow $V_n = nhf/2e$, with $n = 0, 1, 2\cdots$, in which f is the frequency of the applied microwaves, h is Planck's constant, and e is the electronic charge.

The amplitude of the constant-voltage steps is modulated by the microwave power.

The model of a resistively and capacitively shunted junction (RCSJ) can be used to describe the junction behavior according to the equation:

$$I = (\hbar C/2e)d^2\theta/d^2t + (\hbar/2eR)d\theta/dt + I_c \sin\theta, \tag{1}$$

in which I is the current flowing across the junction, $\hbar$ is Planck's constant divided by 2π, C is the junction capacitance, e is tne electronic charge, θ is the phase difference of the superconducting order parameter across the junction, R is the junction capacitance and I_c is the supercurrent of the junction.

If a junction is subjected to microwave irradiation, the microwaves induce an *ac* current I_1 sinwt across the junction, hence I in Eq. (1) can be replaced by $I_0 + I_1 \sin wt$, in which I_0 is the *dc* current flowing across the junction and $I_1 \sin wt$ is induced by microwave irradiation. Eq. (1) becomes

$$I_0 + I_1 \text{ sinwt} = (\hbar C/2e)d^2\theta/d^2t + (\hbar/2eR)d\theta/dt + I_c \sin\theta, \tag{2}$$

Eq. (2) describes a current source RCSJ model. Eq. (2) reverts to a dimensionless equation if we let

$$\beta_c = 2eCI_cR^2/\hbar,\ \omega_0 = 2eI_cR/\hbar,\ \tau = \omega_0 t,\ \Omega = \omega/\omega_0,\ i_0 = I_0/I_c, \text{ and } i_1 = I_1/I_c, \tag{3}$$

Eq. (2) becomes [10]

$$i_o + i_1 \sin\Omega\tau = \beta_c d^2\theta/d^2\tau + d\theta/d\tau + \sin\theta, \tag{4}$$

which is solved numerically to obtain the temporal average of $d\theta/d\tau$ with values of the parameters β_c, i_0, Ω and i_1.

Figure 5a shows the amplitude of the constant-voltage steps in Fig. 4 as a function of the microwave power for $n = 0$ and 1 at f = 7.5 GHz and T = *60* K. The magnitude of the constant-voltage steps was estimated by drawing two parallel lines as shown in the inset of Fig. 5a. For comparison simulated results for the step amplitude as a function of I_1/I_c appear in Fig. 5b for $\Omega = \omega/\omega_0 \sim 0.2$ and β_c = 0 with parameters $f = \omega/2\pi = 7.5$ GHz, and I_c = 2 mA and $R_n = 0.040$ estimated from the $I - V$ curve of the sample at 60 K.

Figure 6a shows the $I - V$ curves for a fixed microwave power (-30 dbm and $f = 7.5$ GHz) at varied applied magnetic fields H = 0, 0.15, 0.19, 0.25, and 0.38 G at T = *70* K. For a fixed microwave power, the amplitude of the constant-voltage steps for n = 0, 1, 2 etc. is modulated with applied magnetic fields. To understand the modulation of the step amplitude by magnetic fields, we consider i_0 in Eq. (4) as a function of the magnetic fields, $i_0(H) = I_0/I_c(H)$. The effect of the magnetic field is to vary I_c of the junction and the

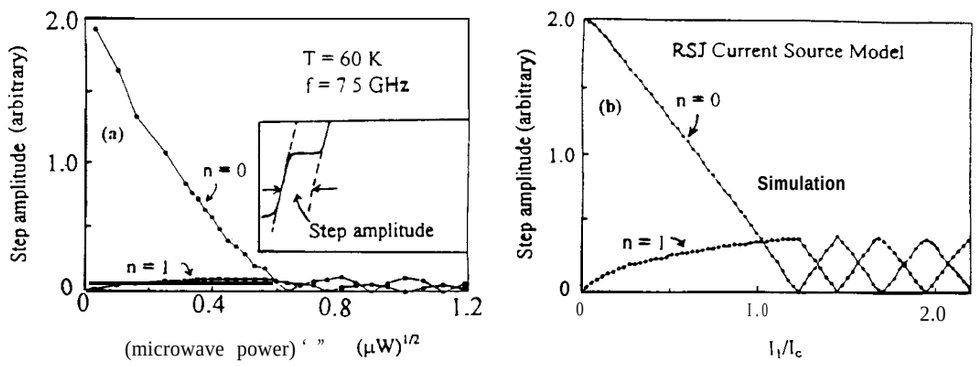

FIG. 5. (a) Step amplitude of constant-voltage steps for a step-edge junction as a function of microwave power for n = 0 and 1 at f = 7.5 GHz and T = 60 K. (b) Simulated results for the step amplitude as a function of I_1/I_c for β_c = 0 and $\Omega = \omega/\omega_0 \sim$ 0.2 with parameters $f = \omega/2\pi =$ 7.5 GHz, and I_c = 2 mA and R_n = 0.040 estimated from the I — V curve of the sample.

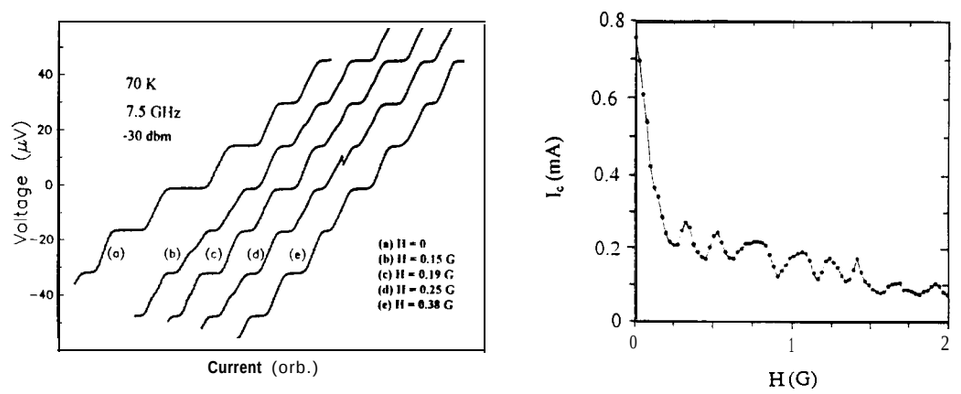

(a) (b)

FIG. 6. (a) I — V curves for a fixed microwave power at various applied magnetic fields at T = 70 K and f = 7.5 GHz. (b) I_c *as* a function of the appled magnetic field at T = *80* K with microwave irradiation at -41 dbm and f = 9 GHz. Modulation of I_c by the magnetic fields is clearly demonstrated.

parameters $\beta_c, \omega_0, \Omega, i_0$ and i_1, therefore giving the step amplitude in Eq. (4). Fig. 6b shows I_c as a function of the applied magnetic field for a stepedge junction (junction width

$\sim 10\ \mu m$) at $T = 80$ K and the microwave irradiation at -41 dbm. As the amplitude of the constant-voltage steps ($n = 0$) is quantitatively equal to $2I_c$, the I_c modulated with magnetic fields in Fig. 6b implies a modulation of the step amplitude ($n = 0$) with magnetic fields under microwave irradiation.

Figure 7 shows the $I-V$ curves for a step-edge junction at $T = 40$ K and $f = 7.5$ GHz under magnetic fields. The applied magnetic field induction coupled to this step-edge junction was 0, 2 and 20 Gauss. The critical current is 14 mA in a zero magnetic field and 3 mA in a magnetic field of $H = 20$ G at $T = 40$ K. Under microwave irradiation (7.5 GHz and -33 dbm) and in a zero magnetic field only three constant-voltage steps are visible in the $I-V$ curves; at $H = 20$ G more than six steps are clearly observed. Hence more constant-voltage steps are observed in magnetic fields than without applied magnetic fields. The effect of the applied magnetic field is to decrease the critical current density of the junction and to enhance the coupling of the microwave power to the junction. A detailed description of the effects of microwave irradiation and magnetic fields on the step amplitude of the constant-voltage steps is reported elsewhere.

In addition to integer constant-voltage steps, half-integer constant-voltage steps were sometimes observed for step-edge Josephson junctions [6] under microwave irradiation. A simulated $I-V$ curve under microwave irradiation appears in Fig. 8 for a junction with

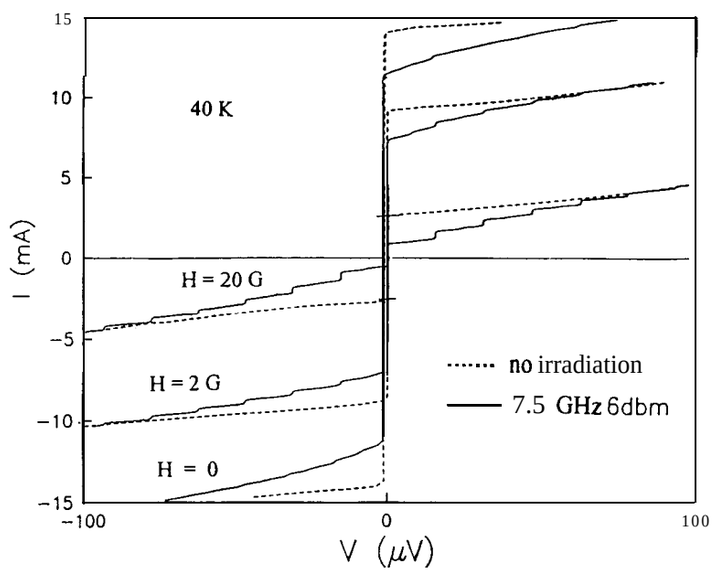

FIG. 7. $I-V$ curves for a step-edge junction at $T = 40$ K and $f = 7.5$ GHz under magnetic fields.

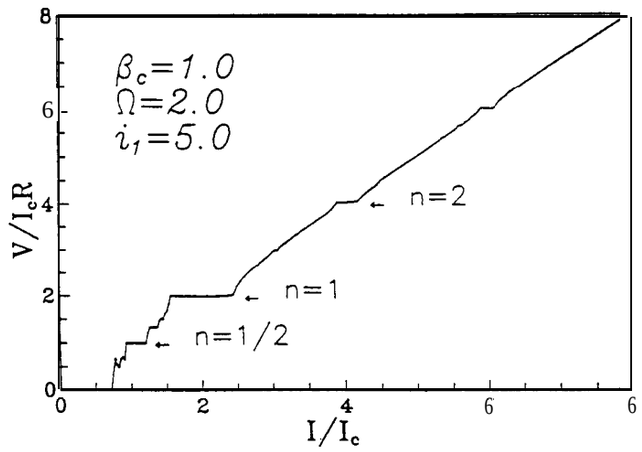

FIG. 8. $I-V$ curve simulated according to a model of an RCSJ current source with the parameters $\beta_c = 1$, $\Omega = 2$ and $i_1 = 5$.

the parameters $\beta_c = 1$, $\Omega = 2$ and $i_1 = 5$. Half-integer constant-voltage steps occur in a single Josephson junction with $\beta_c >> 1$. Our reported stepedge junctions [6] showed no hysteresis ($\beta_c \ll 1$); hence C is completely shorted by the normal resistance R. Thus a large capacitance is less likely to be the cause of the occurrence of half-integer constant-voltage steps. Another possible way for half-integer constant voltage steps to occur in a SQUID and in an applied magnetic field with microwave irradiation is discussed by other authors [10].

Figure 9 shows the $V-\Phi$ curves of SQUID c. SQUID c has a hole area of 5 x 5 μm^2. The peak to peak value in the $V-\Phi$ curves in Fig. 9a corresponds to a flux quantum Φ_0. The voltage of SQUID c reveals that the modulation corresponds to a diffraction pattern caused by a single junction in the SQUID.

Figure 10 shows the $I-V$ curves for a bi-epitaxial YBCO junction on substrate CeO_2/MgO (001) under microwave irradiation. Integer constant-voltage steps are observed and the step amplitude of the constant-voltage steps is modulated with microwave power. The $I-V$ curves of the bi-epitaxial YBCO junctions reveal behaviors predicted according to a model of an RSJ. The reflection high energy diffraction pattern of this bi-epitaxial YBCO junction is shown in Fig. 11. The electron beam was incident on a region near the bi-epitaxial YBCO junction. The distances, d_1 and d_2, are the diffraction spacings corresponding to a YBCO film on the CeO_2 layer and a YBCO film on MgO (001) respectively.

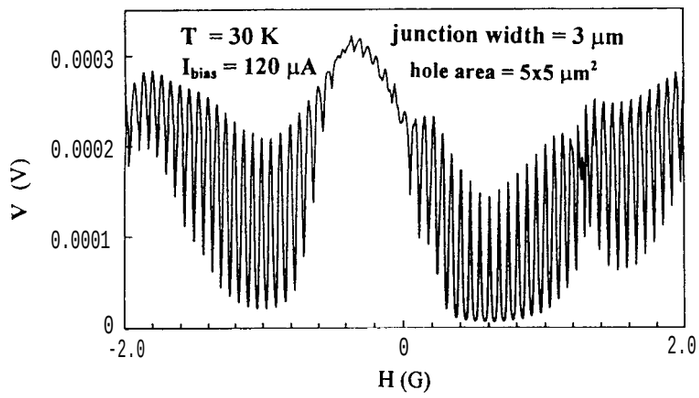

FIG. 9. V $-\Phi$ curves at $T = 30$ K for I_{bias} = 120 μA for SQUID c. The SQUID c has a hole area of 5 x 5 μm^2 and a junction width of 3 μm.

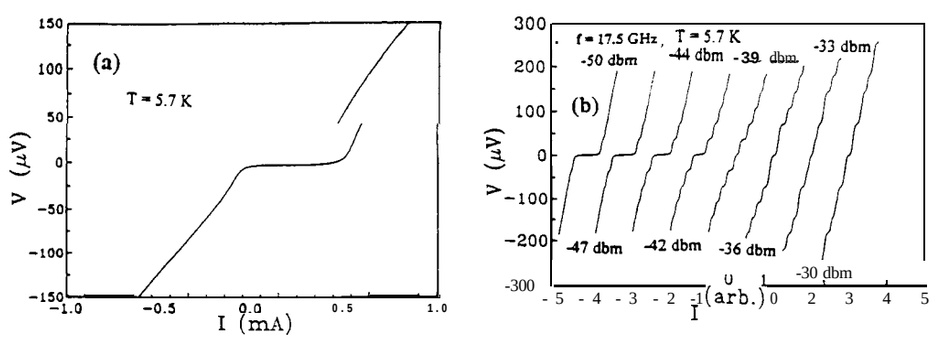

FIG. 10. $I - V$ curves for a bi-epitaxial YBCO junction under microwave irradiation.

The ratio d_1/d_2 (Fig. 11) is $\sim \sqrt{2}$. This suggests that there is a 45° rotation of the crystal a-axis in the YBCO film on the CeO_2 layer with respect to the crystal u-axis of the YBCO film on MgO (001).

IV. JUNCTION CONFIGURATIONS AND TRANSPORT PARAMETERS

High-T, junctions of various types including bi-crystal [1], bi-epitaxial [1,2], step-edge [3-7], superconductor/normal metal/superconductor [8] (SNS) and edge junctions [9] were

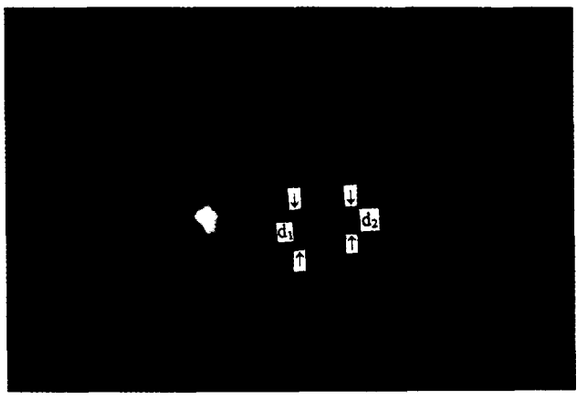

FIG. 11. The reflection high energy diffraction pattern of the bi-epitaxial YBCO junction on substrate CeO_2/MgO (001) at a region near the junction. The ratio d_1/d_2 of the diffraction lines was $\sim \sqrt{2}$. This result mainly suggests that there is a 45° rotation of the crystal a-axis in the YBCO film on the CeO_2 layer with respect to the crystal a-axis of the YBCO film on MgO (001).

intensively investigated both for the essential physics and a design for several stimulating applications [11-13].

A sharp step-edge in the (001) oriented MgO substrates is important in order to fabricate step-edge YBCO junctions of high-quality. If the beam of Ar^+ ions is incident in a direction parallel to the normal of the substrates, a rapid etching rate generally occurs at the edge of the photo-resist, therefore resulting in a step with a slope shown in the inset of Fig. 1. To improve the sharpness of the stepedge of the substrate, it is necessary to tilt the direction of the ion beam with respect to the normal of the substrate. If the ion beam makes an angle α, about $\sim 60°$, with respect to the normal direction of (001) oriented MgO, shown in Fig. la, the normal of the fabricated step is at an angle of $\sim$ 30" with respect to the normal of the substrate (see inset of Fig. 1) as determined from the surface profile. By varying the angle α the critical density of step-edge junctions can be controlled. A typical value of the critical current density of YBCO step-edge junctions [5,6] is $10^4 \sim 10^5$ A/cm^2 at 77 K. The peak-to-pea.k value of the $V-\Phi$ curves [5] for a *dc* SQUID is about 8 μV at 77 K.

Wu et al. [14] reported useful results concerning the in-plane orientational relationships between $LaAlO_3$, $SrTiO_3$, yttria-stabilized zirconia (YSZ), MgO, CeO_2, $BaZrO_3$ and YBCO. A combination of $SrTiO_3$ and MgO films on a Al_2O_3 (R-plane) seed substrate [2] or CeO_2 and YSZ films on (001) oriented MgO seed substrates [15], successfully created 45"

bi-epitaxial YBCO grain-boundary junctions. Hence, a creation of a 45° bi-epitaxial grain boundary in YBCO films by lattice engineering is a distinct method for the fabrication of junctions, SQUID's and arrays. The typical value of the critical current density [2] of bi-epitaxial YBCO junctions is $10^2 \sim 10^3\ \mathrm{A/cm^2}$, whereas the peak-to-peak value of the $V-\Phi$ curves [2] for *dc* SQUID's is about 0.6 μV at 77 K. On increasing the critical current density of the junctions and by decreasing the inductance of the SQUID, the performance of the SQUID is expected to improve at 77 K. The present status of the art of junctions and SQUID's and the extensive activity developed in this topic allow reasonable optimism for the development of bi-epitaxial YBCO junctions.

The critical current density of bi-crystal junctions can be controlled by varying the misorientation angle of the bi-crystal substrate. The advantages of junctions are represented by the readily controlled transport pararneters as a function of the misorientation angle. By varying the misorientation angle, J_c as great as $10^5\ \mathrm{A/cm^2}$ can be produced for bi-crystal YBCO junctions at 77 K. Bi-crystal and step-edge YBCO junctions normally have a larger critical current density, therefore a larger I_cR_n product (I_c is the critical current and R_n is the normal state resistance of the junction), than bi-epitaxial YBCO junctions at the same reduced temperatures.

V. CONCLUSION

$I-$ V curves of YBCO step-edge and bi-epitaxial junctions and SQUID's are reported in this work. The junctions have $I-V$ characteristics well described by the model of an RSJ. The $I-V$ curves under microwave irradiation show constant-voltage steps and the amplitude of the constant-voltage steps is modulated with microwave power. The step amplitude is simulated with the RSJ current source model. The $V-\Phi$ curves of a SQUID under a magnetic field show modulation with a biased current.

ACKNOWLEDGMENT

The authors would like to thank the National Science Council of the Republic of China for financial support under grant number NSC84-2112-M002-20.

REFERENCES

[1] T. Amrein, M. Seitz, D. Uhl, L. Schultz, and K. Urban, Appl. Phys. Lett. 63, 1978 (1993).

[2] K. Char, M. S. Colclough, S. M. Garrison, N. Newman, and G. Zaharchuk, Appl. Phys. Lett. **59**, 733 (1991).

[3] T. Takami, K. Kuroda, K. Kojima, M. Kataoka, J. Tanimura, 0. Wada, and T. Ogama, Jpn. J. Appl. Phys. 32, L583 (1992).

[4] J. Luine, J. Bulman, J. Burch, K. Daly, A. Lee, C. Pettiette-Hall, S. Schwarzbek, and D. Miller, J. Appl. Phys. 61, 1128 (1992).

[5] J. Z. Sun, W. J. Gallagher, A. C. Callengan, V. Foglietti, and R. H. Koch, Appl. Phys. Lett. 63, 1561 (1993).

[6] L. C. Ku, H. M. Cho, J. H. Lu, S. Y. Wang, W. B. Jian, H. C. Yang, and H. E. Horng, Physica C229, 320 (1994).

[7] S. Takana, H. Ttozaki, and T. Nagaishi, Jpn. J. Phys. 32, L662 (1993).

[8] T. Hashimoto, M. Sagoi, Y. Mizutani, J. Yoshida, and K. Mizushima, Appl. Phys. Lett. 60, 1756 (1992).

[9] J. S. Martens, A. Pance, K. Kar, L. Lee, S. Whiteley, and V. M. Hietala, Appl. Phys. Lett. 63, 1681 (1993).

[10] C. Vanneste, C. C. Chi, W. J. Gallagher, A. W. Kleisasser, S. I. Raider, and R. L. Sanstrom, J. Appl. Phys. 54, 242 (1988).

[11] I. S. Gergis, J. T. Cheung, T. N. Trinh, E. A. Sovero, and P. H. Kobrin, Appl. Phys. Lett. 60, 2026 (1992).

[12] L. P. Lee, K. Kar, M. S. Colcough, and G. Zaharchuk, Appl. Phys. Lett. 59, 3051 (1991).

[13] F. Busse, R. Nebel, P. Herzog, M. Darula, and P. Seidel, Appl. Phys. Lett. 63, 1687 (1993).

[14] X. D. Wu, L. L uo, R. E. Muenchausen, K. N. Springer, and S. Foltyn, Appl. Phys. Lett. 60, 1381 (1992).

[15] M. Y. Li, W. J. Chang, H. L. K ao, C. L. Lin, Y. Xu, W. Guan, and M. K. Wu, Chin. J. Phys. 31, 1079 (1993); M. Y. Li, W. J. Chang, H. L. Kao, C. L. Lin, Y. Xu, W. Guan, and M. K. Wu, J. Appl. Phys. 77, 1 (1995).